THE JOURNAL OF BIOLOGICAL CHEMISTRY VOL. 284, NO. 12, pp. 8160–8173, March 20, 2009

Different Transcription Factors Regulate *nestin* Gene Expression during P19 Cell Neural Differentiation and Central Nervous System Development*[S]

Received for publication, July 23, 2008, and in revised form, November 26, 2008 Published, JBC Papers in Press, January 15, 2009, DOI 10.1074/jbc.M805632200

Zhigang Jin[‡], Li Liu[‡], Wei Bian[‡], Yongfeng Chen[‡], Guoliang Xu[§], Leping Cheng[‡1], and Naihe Jing[‡2]

From the [‡]Laboratory of Molecular Cell Biology and [§]State Key Laboratory of Molecular Biology, Institute of Biochemistry and Cell Biology, Shanghai Institutes for Biological Sciences, Chinese Academy of Sciences, 320 Yue Yang Road, Shanghai 200031, China

Nestin is a molecular marker for neural progenitor cells. Rat and human *nestin* genes possess a central nervous system-specific enhancer within their second introns. However, the transcription factors that bind to the *nestin* enhancer have not been fully elucidated. Here, we show that the second intron of the mouse *nestin* gene is sufficient to drive reporter gene expression in the developing nervous system. The core sequence of this central nervous system-specific enhancer localizes to the 3′ 320-bp region. The *cis*-elements for Sox and POU family transcription factors and the hormone-responsive element are essential for *nestin* expression during embryonic carcinoma P19 cell neural differentiation and in the developing chick neural tube. Interestingly, different transcription factors bind to the *nestin* enhancer at different stages of P19 cell neural differentiation and central nervous system development. Sox2 and SF1 may mediate basal *nestin* expression in undifferentiated P19EC cells, whereas Sox2, Brn1, and Brn2 bind to the enhancer in P19 neural progenitor cells. Similarly, *in vivo*, Oct1 binds to the *nestin* enhancer in embryonic day 8.5 (E8.5) mouse embryos, and Oct1, Brn1, and Brn2 bind to this enhancer in E10.5 and E12.5 mouse embryos. Our studies therefore suggest a temporal coordination of transcription factors in determining *nestin* gene expression.

The generation of the three germ layers, the ectoderm, the mesoderm, and the endoderm, is among the earliest and the most fundamental processes underlying animal development. The central nervous system is one of the main derivatives of ectoderm. During development, dorsal ectoderm gives rise to the neural plate, which is later transformed into the neural tube. The neural tube is further subdivided into the fore-, mid-, and hindbrain and the spinal cord along the anterior-posterior axis (1). Different types of neurons in the mature nervous system are generated from pools of mitotic progenitor cells located in the neural tube. Nestin, a type VI intermediate filament protein, is abundant in mammalian neurogenic progenitor cells and has been used as a marker for neural progenitor cells (2–5). To better understand the biology of neural progenitor cells, it is important to study the regulation of the *nestin* gene.

During the development of the central nervous system, early expression of *nestin* mRNA is observed in the neural plate at embryonic day 7.5 (E7.5).[3] At E10.5, *nestin* mRNA is distributed predominantly in the neuroepithelial and radial glia cells of the neural tube of mouse embryos (2). The nestin protein is found in the neural tube prior to neurogenesis, but not post-neurogenesis. When neural progenitor cells (NPCs) in the neural tube differentiate into mature neurons and glial cells, *nestin* expression is down-regulated and replaced by the expression of neurofilament and glial fibrillary acidic protein (2, 6). *nestin* expression is barely detectable in adult central nervous system except for certain proliferative regions, such as the dentate gyrus of the hippocampus and subependymal zones of the brain and spinal cord (2, 7). Nestin expression is induced in response to central nervous system injury and in certain central nervous system tumors (8, 9). Interestingly, the onset of *nestin* expression occurs earlier than the neural plate stage (10). Embryonic stem cells initiate nestin expression immediately after differentiation (11), and pluripotent mouse P19 embryonic carcinoma cells (P19EC) cells maintain basal *nestin* expression (12), whereas both types of cells up-regulate *nestin* expression during their neural differentiation program. These observations suggest that there is a regulation switch for *nestin* expression between pluripotent stem cells and neural progenitor cells.

Compared with nestin expression, little is known about the function of this protein. Recently, nestin has been shown to play an important role in the phosphorylation-dependent disassembly of vimentin intermediate filaments during mitosis and to be

* This work was supported by the National Natural Science Foundation of China (Grants 30623003, 30721065, and 30830034 to N. J.), the National Key Basic Research and Development Program of China (Grants 2005CB522704, 2006CB943902, 2007CB947101, 2008KR0695, and 2009CB941100 to N. J.; Grants 2006CB943900 and 2007CB947102 to L. C.), the National High-Tech Research and Development Program of China (Grant 2006AA02Z186 to N. J.), the Shanghai Key Project of Basic Science Research (Grants 06DJ14001, 06DZ22032, and 08DJ1400501 to N. J.), and the Council of Shanghai Municipal Government for Science and Technology (Grants 05814578 to N. J. and 07pj14098 to L. C.). The costs of publication of this article were defrayed in part by the payment of page charges. This article must therefore be hereby marked "*advertisement*" in accordance with 18 U.S.C. Section 1734 solely to indicate this fact.

[S] The on-line version of this article (available at http://www.jbc.org) contains supplemental Fig. S1 and Table S1.

[1] To whom correspondence may be addressed. Tel.: 86-21-5492-1433; Fax: 86-21-5492-1011; E-mail: lpcheng@sibs.ac.cn.

[2] To whom correspondence may be addressed. Tel.: 86-21-5492-1381; Fax: 86-21-5492-1011; E-mail: njing@sibs.ac.cn.

[3] The abbreviations used are: E, embryonic day; HRE, hormone-responsive element; EC, embryonic carcinoma; NPC, neural progenitor cell; POU, pit, oct, and unc; TK, thymidine kinase; RA, retinoic acid; EMSA, electrophoretic mobility shift assay; NE, nuclear extract; ChIP, chromatin immunoprecipitation; GFP, green fluorescent protein; RT, reverse transcription; qRT, quantitative RT; SF1, steroidogenic factor-1.

a potential target for cdk5 and p35 kinase during development (13, 14). In addition, studies using chick *transitin*, the homolog of mammalian *nestin*, suggest that transitin may physically interact with Numb, determine the intracellular localization of Numb in mitotic avian neuroepithelial cells, and regulate neurogenesis (15).

Because *nestin* expression is closely related to central nervous system development, it is widely used as a specific marker for NPCs in the mammalian nervous system. Studies investigating the transcriptional regulation of the *nestin* gene could enhance our understanding of the regulatory network that links the *nestin* gene and the determination and maintenance of NPCs. The regulation of the rat and human *nestin* genes during development has been investigated in transgenic mice, and data from these mice suggested that the tissue-specific enhancer localized in the second intron of the *nestin* gene is sufficient to drive *nestin* expression in the developing central nervous system (5, 16). The second intron of the *nestin* gene was therefore widely used for deleting gene's expression from the neural progenitor state with the nestin-cre lines (17–20) and labeling the neural progenitor cells using the nestin-GFP transgenic mice (21–23). In this neural enhancer, a POU-binding site is required for general central nervous system expression, and an adjacent hormone response element is necessary for *nestin* expression in the dorsal midbrain and forebrain (24–26). Recently, Tanaka *et al.* (27) demonstrated that members of the Sox and POU family of transcription factors interact synergistically to transactivate the neural enhancer of *nestin* gene *in vitro*, and such an interaction might be involved in the determination of *nestin* expression in neural primordial cells. However, questions such as what transcription factors bind to the *nestin* enhancer to regulate its expression *in vivo*, and whether the same transcription factors regulate *nestin* expression at different stages of central nervous system development, need to be addressed.

Our previous studies described the cloning and expression pattern of the mouse *nestin* gene (28–30) and showed that the transcription factors Sp1 and Sp3 are important for the promoter activity of this gene (31). In this study, we found that a central nervous system-specific enhancer is located in the second intron of the mouse *nestin* gene. This enhancer and its core sequence were able to drive reporter gene expression in the developing nervous system of mouse and chick embryos, as well as during P19 cell neural differentiation. Moreover, different transcription factor complexes bind to the *nestin* enhancer at different stages of P19 cell neural differentiation and central nervous system development. Sox2 and SF1 may mediate basal *nestin* expression in undifferentiated P19EC cells, whereas Sox2, Brn1, and Brn2 regulate the enhancer to increase its expression in P19NPCs. Similarly, *in vivo*, Oct1 binds to the *nestin* enhancer in E8.5 mouse embryos, whereas Oct1, Brn1, and Brn2 bind to this enhancer in the brains of E10.5 and E12.5 mouse embryos.

EXPERIMENTAL PROCEDURES

Transgenic Mice—The second intron of the mouse *nestin* gene was inserted upstream of the basic herpes simplex virus thymidine kinase (tk) promoter in the pSaStk/*lacZ* vector (16). The plasmid was digested with the HindIII restriction enzyme to remove the vector backbone. A purified fragment containing the second intron of the mouse *nestin* gene, the tk promoter, and *lacZ* reporter gene was used for pronuclear injections of fertilized oocytes from ICR mice. Transgenic mice born after the injections were screened by PCR using the primers listed in the supplemental Table S1. One line for pSaStk2In43/1629 and three lines for pSaStk2In1310/1629 were identified as PCR-positive. These clones were propagated through breeding with ICR mice, and the progeny were used for subsequent analyses. One line for pSaStk2In43/1629 and two lines for pSaStk2In1310/1629 had identical patterns of *lacZ* expression throughout the developing central nervous system. Embryos were stained with 5-bromo-4-chloro-3-indolyl-β-D-galactopyranoside as previously described (25).

RNA Analysis—Total RNA was extracted from cultured cells or mouse embryos using TRIzol reagent (Invitrogen). Total RNA (10 μg) from P19 cells during neural differentiation was analyzed by Northern blot as described previously (32). Reverse transcription was performed with 5 μg of total RNA using SuperScript II reverse transcriptase (Invitrogen). The PCR cycling conditions consisted of a denaturation step at 94 °C for 45 s, annealing for 45 s, and extension at 72 °C for 45 s. The primers for each gene are shown in supplemental Table S1. To quantify the relative expression of *nestin* mRNA during neural differentiation of P19 cells, quantitative reverse transcription PCR (qRT-PCR) was performed with the DNA Engine Opticon 2 Real-Time PCR Detection System (Bio-Rad) using Jumpstart Taq Readymix (Sigma) and EvaGreen dye (Biotium, Hayward, CA).

Plasmid Construction—To prepare luciferase reporter constructs for cell transfection, various fragments of the second intron of the mouse *nestin* gene were inserted into the pGL3-Px′ vector (Fig. 2*C*), which was modified within the multiple cloning sites from the pGL3-Promoter (Promega, Madison, WI). These inserts were either prepared by convenient digestions of plasmids or by PCR amplifications. The luciferase reporter construct pNesPE-Luc was used for stable transfection. It was constructed by first amplifying the 1587-bp (43/1629) second intron of the mouse *nestin* gene by PCR to generate the insert. The insert was then cloned into the pNESP-3809/+183 construct, which contains a 4-kb mouse *nestin* gene promoter and a luciferase reporter gene (31). The generation of site-mutated luciferase constructs was performed by PCR using two sets of primers, as described previously (31). All of these constructs were confirmed by enzymatic digestion and DNA sequencing. The primers used to generate the plasmid constructs are listed in supplemental Table S1. To prepare the GFP reporter constructs used for *in ovo* chick embryo electroporation, different fragments of the second intron of the mouse *nestin* gene were inserted into the pxtkEGFP vector. pxtkEGFP was obtained by inserting a KpnI-SacI fragment, which contains the multiple cloning sites in the vector pBluescript SKII into the KpnI and SacI sites in ptkEGFP (33). Site-mutated GFP constructs were generated by the recovery of insert fragments from corresponding luciferase constructs that carried the same site mutations, which were then ligated into the pxtkEGFP vector.

P19 Cell Culture and Retinoic Acid-induced Neural Differentiation—P19 cells were maintained in Dulbecco's modified Eagle's medium/F-12 1:1 medium (Invitrogen) supplemented with 10% fetal bovine serum (HyClone, Logan, UT) at 37 °C in 5% CO_2. P19C6, a subclone of the mouse embryonic carcinoma P19 cell line, was used in this study. Neural differentiation of P19 cells treated with all-*trans*-retinoic acid (RA, Sigma) was performed as described previously (34, 35). Briefly, cells were allowed to aggregate in bacterial grade Petri dishes at a seeding density of 1×10^5 cells/ml in the presence of 1×10^{-6} M RA in 10% fetal bovine serum/α-minimal essential medium (Invitrogen). After 4 days of aggregation, cells were dissociated into single cells and replated on poly-L-lysine-coated tissue culture dishes at a density of 1×10^5 cells/cm^2 in N2 serum-free medium (Dulbecco's modified Eagle's medium/F-12 supplemented with 5 μg/ml insulin, 50 μg/ml human transferrin, 20 nM progesterone, 60 μM putrescine, and 30 nM sodium selenite) supplemented with 1 μg/ml fibronectin. The cells were then allowed to adhere, and they were cultured with replacement of the medium every 48 h. The same protocol was used for neural differentiation of the P19 cell line stably transfected with pNesPE-Luc (named as the NesPEL/P19 cell line).

Cell Transfection and Luciferase Assays—For transient transfection in the P19EC cells, cells were plated onto 24-well plates in 10% fetal bovine serum/Dulbecco's modified Eagle medium/F-12 medium 1 day prior to transfection at a density of 2×10^4 cells/well. For transient transfection in P19NPCs, P19 cells were dissociated into single cells after 4 days of aggregation and replated into 12-well plates in N2 medium 5 h before transfection at a density of 5×10^5 cells/well. Cells were transfected with 0.4 μg of the various luciferase constructs using the Fugene6 reagent (Roche Applied Science), according to the manufacturer's instructions. The pRL-TK plasmid (Promega) containing a *Renilla* luciferase gene driven by the TK promoter was co-transfected with the constructs to normalize the luciferase activity. 40 h later, cell lysates were prepared, and the luciferase activity was measured using the dual reporter assay system (Promega) and a 20/20^n luminometer (Turner Biosystems, Sunnyvale, CA) according to the manufacturer's instructions. All transfections were performed three times in triplicate. For the establishment of the stably transfected cell line NesPEL/P19, P19 cells were co-transfected with 6 μg of pNesPE-Luc, 1.5 μg of pRL-TK, and 2 μg of pPGKneobpA. After selection with G418 for 2 weeks, ~30 G418-resistent clones were picked, expanded, and analyzed for luciferase activity.

In Ovo Chick Embryo Electroporation—Fertilized eggs were obtained from the Shanghai Academy of Agricultural Sciences (Shanghai, China). *In ovo* chick embryo electroporation was performed as previously described (36). Briefly, fertilized eggs were incubated at 38 °C, and the embryos were staged according to Hamburger and Hamilton (37). A DNA solution containing the GFP construct (1.0 μg/μl) as a reporter and pHcRed1-N1 (1.0 μg/μl) as a tracer was injected into the lumen of the closed neural tube of a chick embryo at HH stage 10 and electroporated into cells on one side of the neural tube by electrodes flanking the embryo. A square wave current (six 30-ms pulses of 25 V) was generated using a BTX ECM830 Electro Square Porator (Genetronics, San Diego, CA) connected to 4-mm platinum electrodes. Embryos were collected after a 24-h incubation (HH stage 17), fixed in 4% paraformaldehyde for 1 h at 4 °C, and they were examined with a fluorescence dissection microscope (Leica, Wetzlar, Germany). Neural tubes expressing HcRed1 were removed from the embryos, equilibrated in 20% sucrose overnight, embedded in Tissue-Tek OCT compound (Leica), and sectioned at a thickness of 10 μm. Fluorescence was visualized and photographed using the TCS SP2 Confocal Microscopy System (Leica).

Electrophoretic Mobility Shift Assays—Nuclear extracts (NE) from P19 cells and mouse embryos were prepared as described previously (31). NE (~5 μg) was preincubated with 2 μg of poly(dG-dC) (Amersham Biosciences) and 10 μg of bovine serum albumin on ice for 30 min in 5 × binding buffer containing 50% glycerol, 60 mM HEPES, pH 7.9, 20 mM Tris-HCl, 300 mM KCl, 5 mM EDTA, and 5 mM dithiothreitol. A ^{32}P-labeled DNA probe was added to the binding reaction mixture and incubated at 25 °C for 30 min. Competition experiments were performed by preincubation of a 100-fold molar excess of unlabeled probe together with NE. For supershift assays, specific antibodies were added to the reaction mixture before the addition of labeled probe. DNA-protein complexes were fractioned on a pre-run non-denaturing 6% polyacrylamide gel and subjected to electrophoresis in 0.5× TBE buffer (45 mM Tris-boric acid pH 8.0, and 1 mM EDTA). The gels were dried and exposed to x-ray film with an intensifying screen at −80 °C. The oligonucleotide sequences of the probes and competitors are reported in supplemental Table S1. The following antibodies were used for supershift assays: rabbit anti-human Oct1 (sc-232X, Santa Cruz Biotechnology, Santa Cruz, CA), rabbit anti-human Oct2 (sc-233X), goat anti-human Oct4 (sc-8628X), goat anti-human Oct6 (sc-11660X), goat anti-human Brn1 (sc-6028X), goat anti-human Brn2 (sc-6029X), goat anti-human Sox2 (sc-17320X), and rabbit anti-mouse SF1 (38).

Chromatin Immunoprecipitation—Chromatin immunoprecipitation (ChIP) was performed according to the manufacturer's protocol (Upstate Biotechnology, Charlottesville, VA) with minor modifications. Cellular protein-DNA complexes were cross-linked by incubating the cells in 1% formaldehyde for 10 min at room temperature. The reaction was stopped with the addition of 125 mM glycine. After washing with cold phosphate-buffered saline, the cells were lysed with cell lysis buffer (10 mM HEPES, pH 7.9, 0.5% Nonidet P-40, 1.5 mM $MgCl_2$, 10 mM KCl, 0.5 mM dithiothreitol, 1 mM phenylmethylsulfonyl fluoride, and protease inhibitor mixture (Roche)) for 10 min at 4 °C. The pellets were resuspended in SDS lysis buffer (1% SDS, 10 mM EDTA, 50 mM Tris-HCl pH 8.0, 1 mM phenylmethylsulfonyl fluoride, and protease inhibitor mixture) and incubated for 20 min at 4 °C. Resuspended cells were sonicated with a Bioruptor (Diagenode, Liège, Belgium), and debris was removed by centrifugation. The supernatants were diluted 10-fold with dilution buffer (16.7 mM Tris-HCl, pH 8.0, 0.01% SDS, 1.1% Triton X-100, 1.2 mM EDTA, 167 mM NaCl, 1 mM phenylmethylsulfonyl fluoride, and protease inhibitor mixture) and then precleared with 40 μl of protein A/G-Sepharose slurry (Upstate) for 1 h at 4 °C. Immunoprecipitation was performed with 4 μg of the specific antibody (the same antibodies were used as in the EMSA assays) incubated overnight at 4 °C. Normal rabbit or

goat IgG was used as a negative control. Antibody complexes were pulled down for 2 h with 40 μl of protein A/G-Sepharose slurry. The Sepharose beads were then collected and washed sequentially for 5 min in low salt buffer (50 mM HEPES, pH 7.9, 0.1% SDS, 1% Triton X-100, 1 mM EDTA, 140 mM NaCl, 0.1% deoxycholate), high salt buffer (50 mM HEPES, pH 7.9, 0.1% SDS, 1% Triton X-100, 1 mM EDTA, 500 mM NaCl, 0.1% deoxycholate), and LiCl buffer (20 mM Tris-HCl, pH 8.0, 1 mM EDTA, 250 mM LiCl, 0.5% Nonidet P-40, 0.5% deoxycholate) three times. Beads were washed twice with 1× TE buffer and extracted with elution buffer (1% SDS, 100 mM $NaHCO_3$). The eluates were heated at 65 °C for at least 5 h to reverse the cross-links. The DNA fragments were purified by phenol extraction, ethanol precipitation, and quantified by quantitative PCR using the DNA Engine Opticon 2 Real-Time PCR Detection System (Bio-Rad). The amounts of immunoprecipitated DNA were calculated by comparison to a standard curve generated by serial dilutions of input DNA, dividing the values obtained with normal rabbit or goat IgG. The data were plotted as the mean of at least two independent ChIP assays and three independent amplifications. The primer sets used to amplify the second intron of the mouse *nestin* gene were NesEn1 (second intron, 1311/1510, 200 bps) and NesEn2 (second intron, 1290/1510, 221 bps). The primer sets used as control to amplify the promoter of the mouse *nestin* gene were NesPro1 (5′ flanking, −40/+187, 227 bps). The primer sequences are listed in supplemental Table S1.

Immunofluorescent Staining—Immunofluorescent staining was performed as described previously (34). The primary antibodies and their final concentrations were as follows: rabbit anti-human Oct1 (1:1000, Santa Cruz Biotechnology), mouse anti-human Oct4 (1:200, Santa Cruz Biotechnology), goat anti-human Brn1 (1:1000, Santa Cruz Biotechnology), goat anti-human Brn2 (1:1000, Santa Cruz Biotechnology), rabbit anti-mouse Sox2 (1:200) (27), rabbit anti-mouse SF1 (1:1000) (38), rabbit anti-mouse nestin (1:200) (39), mouse anti-rat nestin (1:200, BD Biosciences, San Jose, CA). Fluorescein isothiocyanate- and Cy3-conjugated secondary antibodies were obtained from Jackson ImmunoResearch Laboratories (West Grove, PA). The fluorescence was visualized and photographed on a BX51 fluorescence microscope (Olympus, Tokyo, Japan) and a TCS SP2 Confocal Microscope (Leica).

RESULTS

The Second Intron of the Mouse nestin Gene Contains a Central Nervous System-specific Enhancer—Previous studies have shown that the second introns of the rat and human *nestin* genes contain a central nervous system-specific enhancer (5, 16). To examine if the second intron of the mouse *nestin* gene also contains this central nervous system-specific enhancer, we generated transgenic mice with the pSaStk2In43/1629 construct, which contains the second intron of the mouse *nestin* gene, a tk promoter, and *lacZ* reporter. At embryonic day (E) 12.5, the pSaStk2In43/1629 transgenic embryos exhibited *lacZ* expression in most parts of the developing central nervous system, including the spinal cord, myelencephalon, metencephalon, mesencephalon, diencephalon, and telencephalon (Fig. 1, *A–C*). Interestingly, about one-third of the *lacZ*-positive

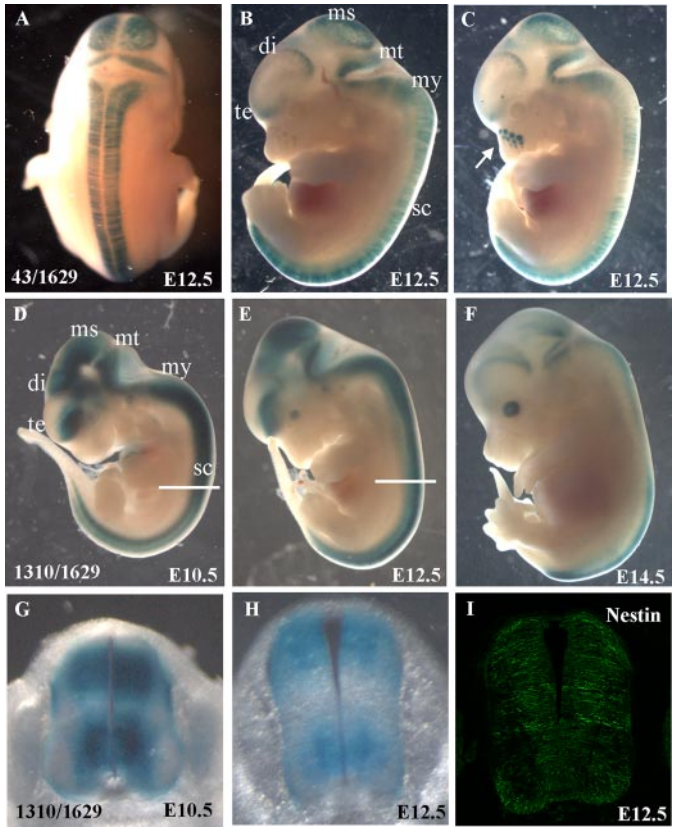

FIGURE 1. ***LacZ* expression in transgenic embryos carrying mouse *nestin* second intron-*lacZ* constructs.** Whole mount *lacZ* staining was performed using transgenic embryos expressing the pSAStk2In43/1629 construct at E12.5 (*A–C*) and the pSAStk2In1310/1629 construct at E10.5 (*D*), E12.5 (*E*), and E14.5 (*F*). *LacZ* was expressed in the spinal cord (*sc*), myelencephalon (*my*), metencephalon (*mt*), mesencephalon (*ms*), diencephalon (*di*), and telencephalon (*te*) (*B–F*). *A* is the dorsal view, and *B* and *C* are the lateral views of the same embryo. *LacZ* expression in whisker follicle sheath progenitor cells is indicated by the *arrow* (*C*). *G* and *H*, the transverse sections of the lumbar spinal cord from pSAStk2In1310/1629 transgenic mice, indicated by *lines* in the area of *D* and *E*, respectively. *LacZ* expression was restricted to both sides of neural tube (*G* and *H*). *I*, endogenous nestin expression in the neural tube was examined by immunostaining on a transverse section from wild-type mouse embryos at E12.5.

embryos exhibited *lacZ* expression in the whisker follicle sheath progenitor cells (Fig. 1*C*). No other area of expression was reproducibly observed. These results demonstrate that, like the rat and human *nestin* genes (2, 5, 16), the second intron of the mouse *nestin* gene confers a spatial and temporal pattern of expression in the developing central nervous system that is similar to that of the endogenous *nestin* gene.

Nestin Expression Is Regulated by the Second Intron during P19 Cell Neural Differentiation—RA-induced P19 cell neural differentiation is a well established *in vitro* model to study the molecular mechanisms involved in the development of mammalian central nervous system (40–43). This process may be divided into two stages: the induction stage, where P19 cells were aggregated and induced by RA for 4 days, and the differentiation stage, in which the induced P19 cells were replated as single cell suspensions and differentiated for up to 2 weeks (40). In this study, we named the days after aggregation and RA treatment as A1, A2, A3, and A4 and the days after replating as R1, R2, R3, etc. Northern blotting was used to detect *nestin* expression during neural differentiation of the P19 cells (Fig. 2*A*, *left*

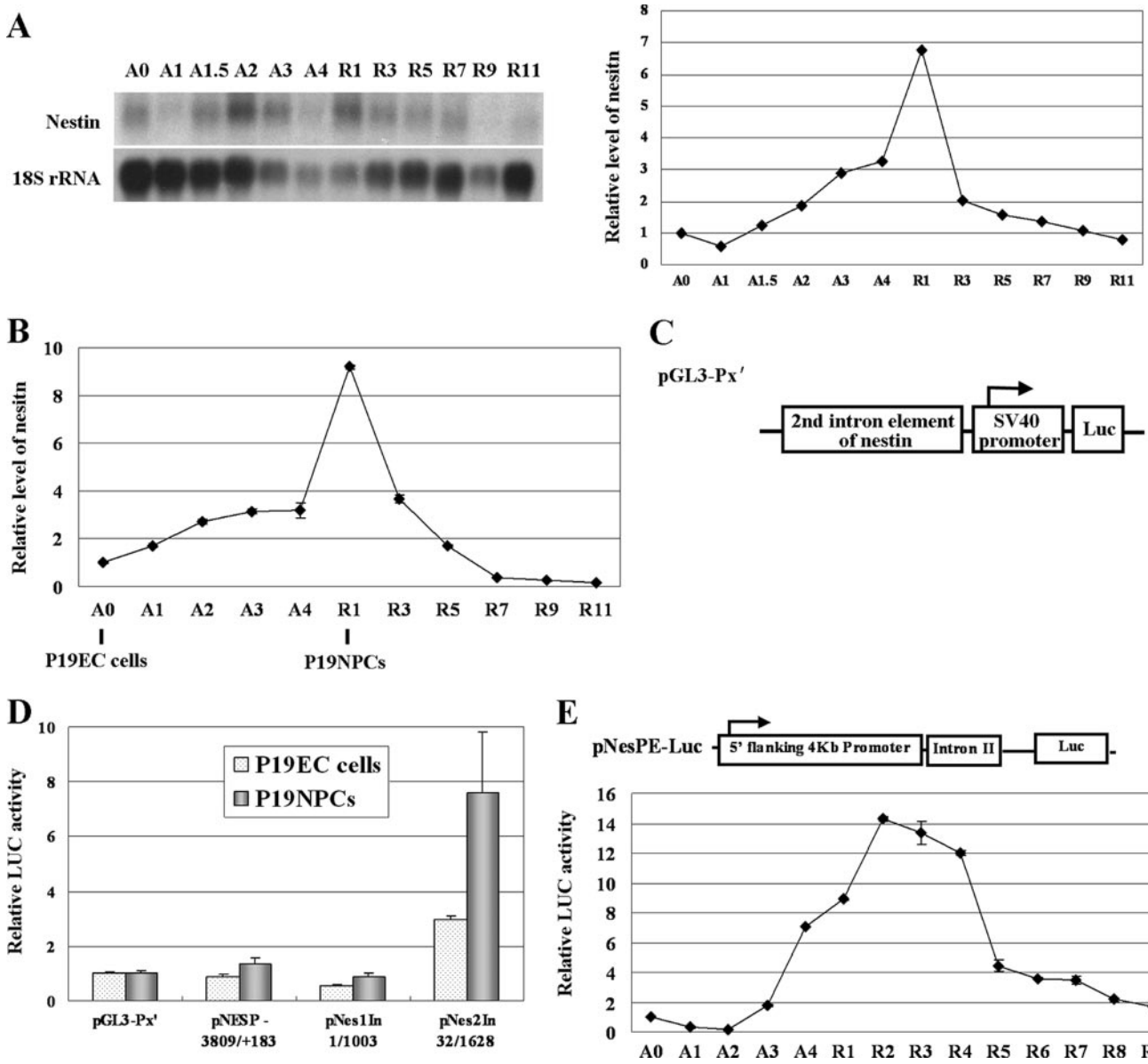

FIGURE 2. **The second intron of the mouse *nestin* gene directed *nestin* expression during RA-induced P19 neural differentiation.** *A*, Northern blot analysis of *nestin* mRNA expression. Total RNA extracted from P19 cells during RA-induced neural differentiation was used for Northern blotting. 18 S rRNA was used as a control. Semi-quantitative analysis of the Northern blot results is shown in the *right panel*. *B*, qRT-PCR analysis of *nestin* mRNA expression. Total RNA extracted from P19 cells during neural differentiation was analyzed using qRT-PCR with primers specific for mouse *nestin* and *β-actin*. The amount of *nestin* mRNA was normalized to that of *β-actin*, and the value in undifferentiated P19EC cells (A0) was designated as 1. *C*, *diagram* of the pGL3-Px′ vector. Various fragments of the second intron of the mouse *nestin* gene were inserted upstream of the SV40 promoter. *D*, luciferase constructs containing the 5′ upstream promoter (pNESP-3809/+183), the first intron (pNes1In 1/1003), or the second intron (pNes2In32/1628) of the mouse *nestin* gene were transiently transfected into P19EC and P19NPC cells. The activity of each construct is shown relative to that of the pGL3-Px′ vector, which contains a SV40 promoter. Values were normalized for transfection efficiency by co-transfection with a *Renilla* luciferase expression plasmid, and they are shown as means ± S.D. for three independent experiments. *E*, luciferase activity during neural differentiation of NesPEL/P19 cells. P19 cells were transfected with pNesPE-Luc, pRL-TK, and pPGKneobpA and selected with G418. A stable cell line, NesPEL/P19-E, was induced for neural differentiation, and the luciferase activity was measured. Firefly luciferase activity was normalized with that of *Renilla* luciferase. Luciferase activity in undifferentiated NesPEL/P19-E cells (A0) was designated as 1, and the relative luciferase activity of NesPEL/P19-E cells at different stages was then calculated.

panel). We found that *nestin* mRNA was present at low levels in undifferentiated P19 cells (A0), and the expression was up-regulated upon RA induction, with an expression peak at replating day 1 (R1) (Fig. 2*A*, *right panel*). As neural differentiation proceeded, *nestin* expression was down-regulated to the basal level at R9. Consistently, the qRT-PCR analysis also showed a transient increase in *nestin* mRNA, with an expression peak at R1 (Fig. 2*B*). These results suggest that the *nestin* gene has a very similar expression pattern in P19 cell neural differentiation and central nervous system development *in vivo* (2), suggesting that this process could be used as an *in vitro* system to study transcriptional regulation of the *nestin* gene during central nervous system development. Based on this observation, we proposed that the non-induced P19EC cells (A0) represented the pluripotent stem cells and that the replating day 1 or 2 (R1 or R2) RA-induced P19 cells (P19NPCs) represented the neural progenitor cells of the developing central nervous system (Fig. 2*B*).

To identify the regulatory sequence of the *nestin* gene responsible for *nestin* expression during P19 cell neural differentiation, we scanned the genomic sequence of the mouse *nestin* gene using a luciferase reporter assay in P19EC cells and P19NPCs. The second intron (pNes2In32/1628) increased the luciferase activity by ~3-fold in P19EC cells, and up to 8-fold in P19NPCs compared with the control pGL3-Px′ vector, whereas the 5′ upstream promoter (pNESP −3809/+183) and the first intron (pNes1In1/1003) failed to show any enhancer activity (Fig. 2, *C* and *D*). To confirm the function of the second intron, we generated a pNesPE-Luc construct containing a 4-kb upstream region and the second intron of *nestin* gene, and established stable P19 cell lines with this construct (NesPEL/P19 cells). Representative clones, such as NesPEL/P19-E, were induced for neural differentiation, and the luciferase activity was measured. The expression of the luciferase reporter also transiently increased along with neural differentiation and had an expression peak at R2, 1 day later than the *nestin* mRNA peak at R1 (Fig. 2*E*). Similar results were obtained from other clones of the NesPEL/P19 cells (data not shown). In conclusion, the second intron of mouse *nestin* gene is responsible for regulation of *nestin* expression during P19 cell neural differentiation.

Identification of the Minimal Enhancer and cis-Elements—To identify the core sequence(s) in the second intron of the mouse *nestin* gene, a series of deletion constructs was transiently transfected into P19EC cells and P19NPCs (Fig. 3*A*). We found that a 320-bp region at the 3′ end of the second intron (pNes2In1310/1629) displayed enhancer activity comparable to that of the full-length second intron (pNes2In32/1629) in both P19EC cells and P19NPCs. The constructs lacking this 320-bp fragment showed a significant loss of enhancer activity in P19EC cells and P19NPCs, confirming the importance of this region to the augmented enhancer activity during neuronal differentiation. We further divided this 320-bp fragment into a 5′-proximal 151-bp fragment (pNes2In1310/1460) and a 3′-proximal 171-bp fragment (pNes2In1459/1629) and found that the upstream 151-bp fragment possessed full enhancer activity in P19EC cells and partial activity in P19NPCs. However, the downstream 171-bp region had no enhancer activity. These results suggest that the 151-bp fragment (1310/1460) contains the majority, but probably not all, of the regulatory elements (Fig. 3*A*). Some other elements in the 320-bp region may confer either repression or activation activity in P19EC cells or P19NPCs, although these experimental states will not be represented as the physiological state by the reporter vectors (Fig. 3*A*).

To validate the enhancer activity of this 320-bp region *in vivo*, we generated the pSaStk2In1310/1629 construct and examined the pattern of *lacZ* expression in the transgenic mice. At E10.5 and E12.5, this 320-bp minimal enhancer could also initiate *lacZ* expression that was restricted to the proliferating central nervous system progenitor cells (Fig. 1, *D* and *E*). Although the enhanced *lacZ* staining was observed on the 320-bp enhancer transgenic mice *versus* the full-length second intron enhancer transgenic mice, the central nervous system-specific pattern was the same. As these two lines were produced at different time, the intensity difference may result from difference in the integration of the 320-bp region and the full-length second intron enhancer. For the human or rat *nestin* enhancers, the conserved regions of the second intron of the *nestin* genes have been shown to function indistinguishably as the full-length second intron (5, 16). In sections of transgenic embryos at E10.5 and E12.5, intense *lacZ* expression was observed proximal to the ventricular zone of the neural tube (Fig. 1, *G* and *H*), similar to the pattern of endogenous *nestin* expression (Fig. 1*I*). At E14.5, weak expression could be detected in relatively confined regions (Fig. 1*F*), consistent with the observation that most of the NPCs have differentiated into neurons and there is a decrease in *nestin* expression (2). Therefore, the central nervous system-specific enhancer of mouse *nestin* gene resides in the 3′ 320-bp region of the second intron.

The 320-bp minimal enhancer contains several putative *cis*-elements, such as HRE and binding sites for Sox and the POU family transcription factors (24, 27, 44, 45). By carefully examining this sequence, we also found two overlapping binding sites for the steroidogenic factor-1 (SF1, also known as Ad4BP and NR5A1), which are in perfect agreement with the consensus sequence for SF1 (Fig. 3*B*) (46). It is noteworthy that the binding sites for Sox, POU, HRE, and SF1 factors in the enhancer are conserved among the mouse, rat, and human *nestin* genes (Fig. 3*C*). The POU site and HRE from the three species are perfectly conserved (no mismatch). The SOX and SF1 sites are also perfectly conserved between the mouse and the rat *nestin* genes, either of which has two bases mismatch with the human counterpart. Nevertheless, the sequence of SOX site of the human *nestin* gene is also a good binding site for SOX (47), and the SF1 site of the human *nestin* gene has only one base mismatch with SF1 consensus binding sites (46). To further evaluate the importance of these regulatory elements, reporter constructs carrying mutations in the minimal enhancer element were generated and transfected into P19EC and P19NPC cells. As shown in Fig. 3*D*, mutations in the Sox-binding site (pNes2InSoxm) or POU-binding site (pNes2InPOUm), as well as double mutations in both sites (pNes2InSoxmPOUm), could attenuate luciferase activity in both P19EC cells and P19NPCs. Similar results were obtained when the HRE (pNes2InHREm) was mutated. Interestingly, mutation of SF1-binding sites caused a severe decrease in luciferase activity in P19EC cells, but not in P19NPCs. Taken together, these results demonstrate that Sox- and POU-binding sites, and HRE are important *cis*-elements for *nestin* enhancer activity in P19EC and P19NPC cells and are responsible for the activation of the enhancer during neural differentiation, while SF1-binding sites are important in P19EC cells.

The Expression Pattern of Putative Transcription Factors during P19 Cell Neural Differentiation—To identify the putative transcription factors involved in *nestin* gene regulation, RT-PCR analysis was used to examine the expression patterns of the SF1, Sox, and POU family members during P19 cell neural differentiation (Fig. 4*A*). The results showed that *SF1* and *Oct4* were expressed in the undifferentiated P19EC cells (A0), and the levels of their expression began to decrease immediately after RA induction. The transcripts of *Brn1*, *Brn2*, *Sox1*, and *Sox11* could not be detected in P19EC cells; however, the expressions of these genes were induced at A1 or A2, and they continued to be expressed in P19NPCs from R1 to R3. *Sox2* was weakly expressed in P19EC cells, and it was transiently up-regulated during neural

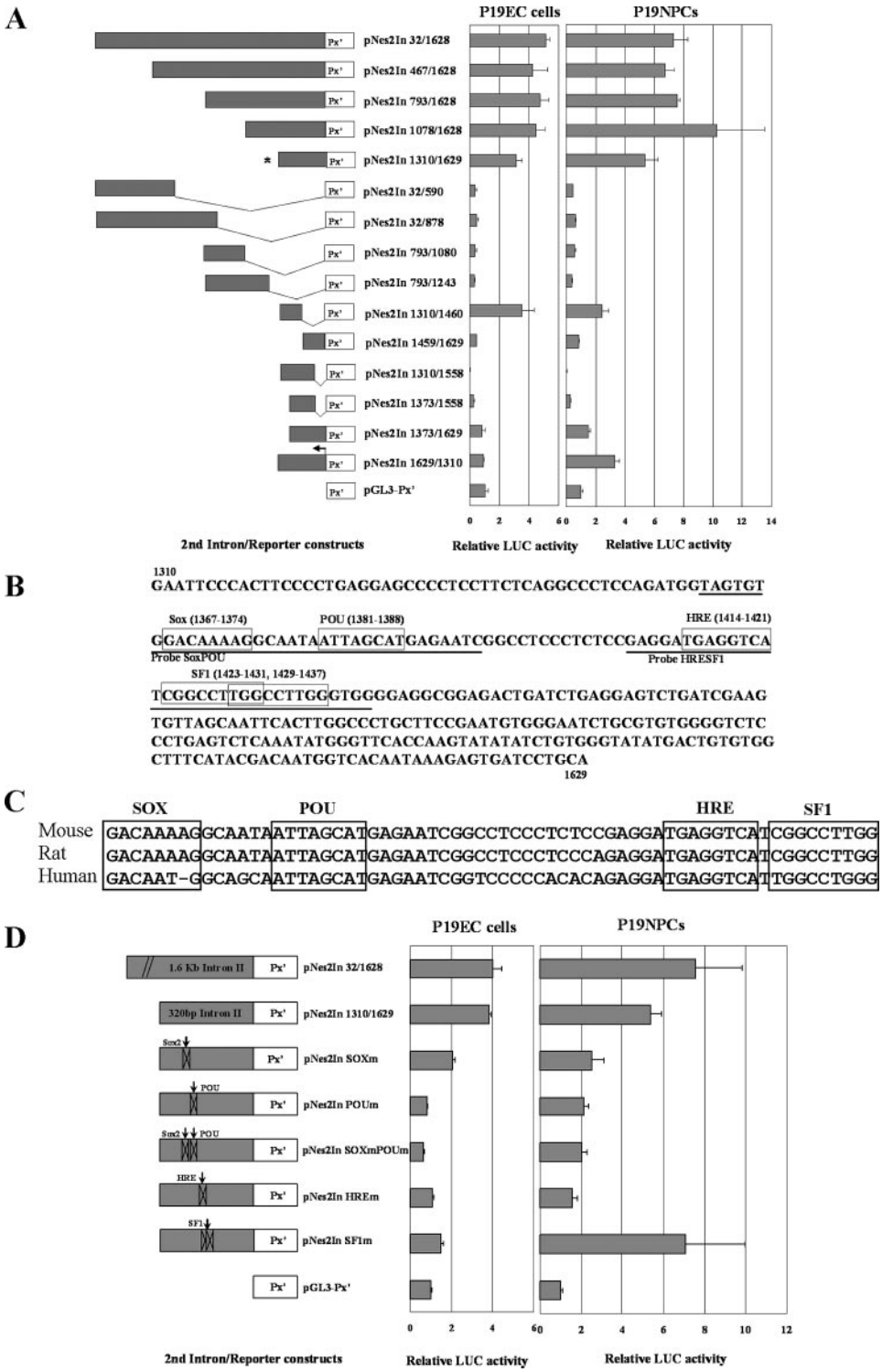

FIGURE 3. **Identification of the core sequence and functional *cis*-elements in the second intron of the mouse *nestin* gene.** *A*, the minimal enhancer region was localized to the 3′ 320 bp (1310/1629) region of the second intron. P19EC cells or P19NPCs were transfected with deletion constructs as indicated in the *left panel*, and the luciferase activity was determined. The minimal enhancer containing 3′ 320 bp is indicated by an *asterisk*. *B*, potential *cis*-elements in the 3′ 320 bp of the second intron. The position of the first nucleotide of the second intron was designated as 1. The consensus sequences of putative *cis*-elements are shown in *boxes*. *C*, alignment of the nucleotide sequence, which contains the binding sites for Sox, POU, HRE, and SF1 factors in the 320-bp region with its counterparts in the rat and human *nestin* genes. *D*, identification of functional *cis*-elements. P19EC or P19NPC cells were transfected with site-mutated constructs as indicated in the *left panel*, and the luciferase activity was determined. The activity of each construct was shown relative to that of the enhancer-less pGL3-Px′ vector. Values were normalized for transfection efficiency by co-transfection with a *Renilla* luciferase expression plasmid, and they are shown as means ± S.D. for three independent experiments.

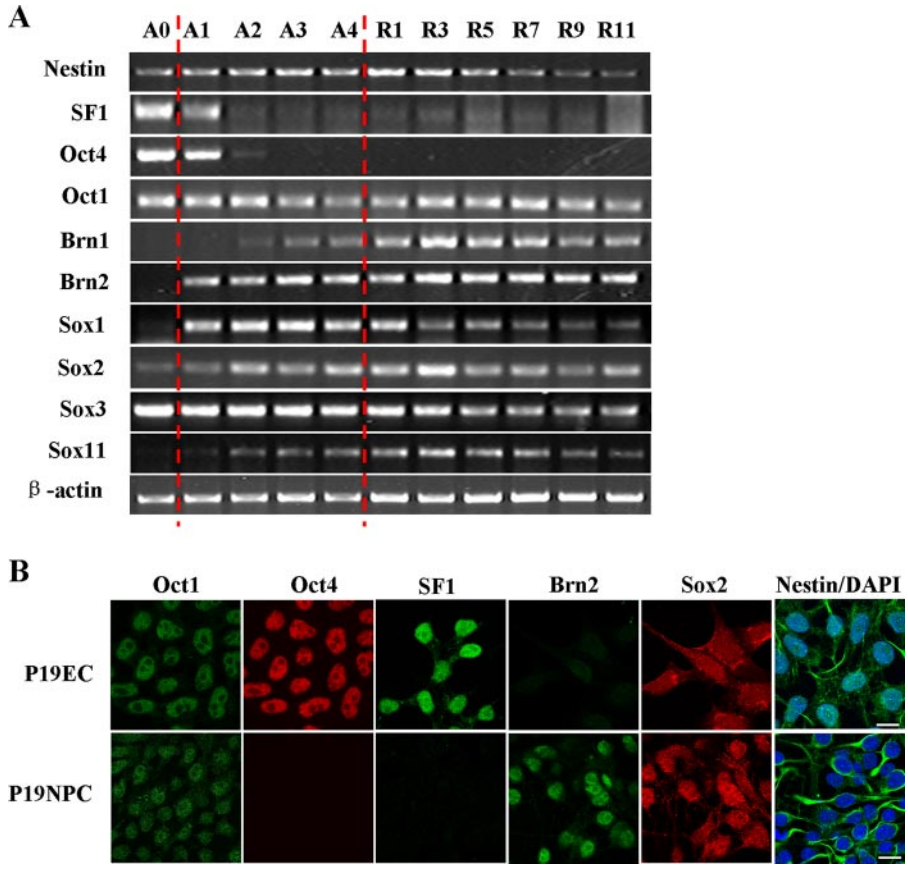

FIGURE 4. **Expression of SF1, Sox, and POU family transcription factors during neural differentiation of P19 cells.** *A*, RT-PCR analysis of expression of transcription factors during neural differentiation of P19 cells. Total RNA extracted from P19 cells during RA-induced neural differentiation was used for RT-PCR. *β-actin* was used as a control. *B*, immunostaining of transcription factors in P19EC and P19NPC cells. For P19NPCs, P19 cells after 4 days of aggregation were dissociated into single cells and replated in N2 medium. At day 2 after replating (*R2*), the cells were analyzed by immunostaining. *Bar*, 10 μm.

differentiation, which was similar to the pattern of *nestin* expression observed. In contrast to the other factors, *Oct1* and *Sox3* were continuously expressed throughout this process. We could not detect the expression of thyroid transcription factor-1 (*TTF1*, also known as *Nkx2.1*) and *Brn4* in either undifferentiated or differentiating P19 cells (data not shown).

Immunostaining was used to confirm the expression of putative transcription factors in P19EC cells and P19NPCs (Fig. 4*B*). Consistent with the RT-PCR results, the patterns of Oct4 and SF1 protein expression in P19EC and P19NPC were observed in the nuclei of P19EC cells, but not in P19NPCs. However, the Brn1 (data not shown) and Brn2 proteins were found in the nuclei of P19NPCs, but not in P19EC cells. The Oct1 and Sox2 proteins were expressed in both P19NPCs and P19EC cells. Taken together, these results suggest that the putative transcription factors expressed in P19EC cells include Oct1, Oct4, Sox2, Sox3, and SF1, and putative transcription factors expressed in P19NPCs are Oct1, Brn1, Brn2, Sox1–3, and Sox11.

The nestin Enhancer Is Occupied by Different Transcription Factors during P19 Cell Neural Differentiation—EMSA was utilized to characterize the transcription factors that potentially bind to the minimal enhancer of the mouse *nestin* gene. The 1367/1437 region within the 320-bp minimal enhancer, which contains all four *cis*-elements (Fig. 3*B*), was divided into two oligonucleotides for EMSA: oligonucleotides 1360–1395 as the Sox-POU probe and 1409–1441 as the HRESF1 probe (Fig. 3*B*, *underlined*). A time-course analysis of the proteins that bound to the Sox and POU *cis*-elements was first performed using the radiolabeled Sox-POU probe with the same quantity of P19 cell NE prepared at different time points of neural differentiation. Poly(dG-dC) was used instead of poly(dI-dC) as a nonspecific DNA competitor to allow binding by high-mobility group box proteins (48). Two prominent complexes (*bands 1* and *2*) were found in extracts from P19EC cells at A0 (Fig. 5*A*, *lane 1*); complex 2 disappeared after A2, while complex 1 became weaker but was still detectable until R5 (Fig. 5*A*, *lanes 3–7*). Another two complexes (bands 3 and 4) were obvious at A4, and they peaked by R1 and R3, decreasing and eventually disappearing after R7 (Fig. 5*A*, *lanes 5–9*). The complexes 1–2 in P19EC cells and complexes 1, 3, and 4 in P19NPCs were specific to particular DNA sequences since they were successfully competed away with 100-fold molar excess of non-radiolabeled probe (Fig. 5*B*, *lanes 3* and *10*) but not with an irrelevant competitor such as CIE (*cis*-inducible element) (Fig. 5*B*, *lanes 2* and *9*). As a control, we also used the POU-binding site in the upstream enhancer of the mouse *Sox2* gene, POU1(*Sox2*) (49), which also competed away these bands in P19EC and P19NPC cells (Fig. 5*B*, *lanes 4* and *11*). To identify the important binding sites in this SoxPOU probe, DNA probes with mutations in the Sox (SoxmPOU) or POU sites (SoxPOUm) or mutations at both sites (SoxmPOUm) were used as competitors. The SoxmPOU probe effectively abolished the formation of *bands 1–2* in P19EC cells (Fig. 5*B*, *lane 5*), as well as *bands 1*, *3*, and *4* in P19NPCs (Fig. 5*B*, *lane 12*), whereas the other two probes failed to compete away any band (Fig. 5*B*, *lanes 6* and 7, and *13* and *14*). Consistently, the radiolabeled SoxmPOU probe could form complexes with the same mobility as the wild-type probe in P19 cell NE, although no complexes were formed with the radiolabeled SoxPOUm or SoxmPOUm probes (data not shown). These observations suggest that different transcription factors are specifically recruited to POU factor-binding sites in the *nestin* gene minimal enhancer to generate complexes 1 and 2 in P19EC cells and complexes 1, 3, and 4 in P19NPCs, respectively.

To identify the transcription factors present in the complexes 1–4, supershift assays were performed (Fig. 5*C*). In P19EC cells, complex 1 could be supershifted by an Oct1 antibody, and complex 2 was diminished by an Oct4 antibody,

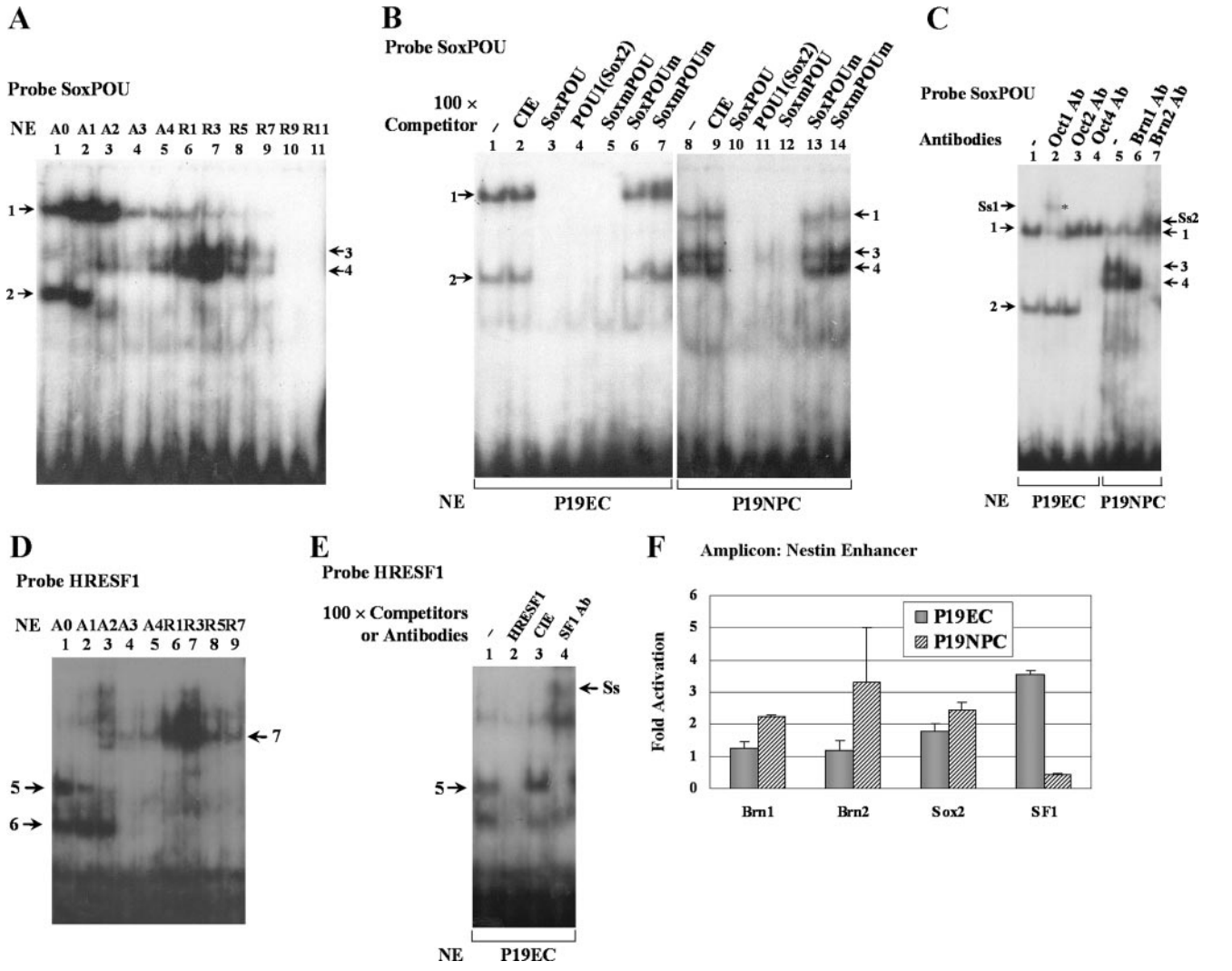

FIGURE 5. **Different transcription factors are recruited to the *nestin* enhancer during neural differentiation of P19 cells.** *A*, a ^{32}P-labeled SoxPOU probe (1360/1395) was incubated with NE from P19 cells. EMSA was performed with the same amount of NE from P19 cells (5 μg). Specific gel-shifted bands (*1–4*) formed in P19EC cells and P19NPCs are indicated by *arrows*. *B*, ^{32}P-labeled SoxPOU probe was incubated with NE from P19EC cells (*lanes 1–7*) or P19NPCs (*lanes 8–14*). The competition experiment was performed with 100-fold excess of unlabeled non-relevant probe CIE (*lanes 2* and *9*), SoxPOU probe (*lanes 3* and *10*), POU1(Sox2) probe (*lanes 4* and *11*), Sox-mutated probe SoxmPOU (*lanes 5* and *12*), POU-mutated probe SoxPOUm (*lanes 6* and *13*), or a probe with both the Sox and POU sites mutated probe SoxmPOUm (*lane 7* and *14*). *C*, a ^{32}P-labeled SoxPOU probe was incubated with NE from P19EC cells (*lanes 1–4*) or P19NPCs (*lanes 5–7*). The supershift assay was performed with an antibody against Oct1 (*lane 2*), Oct2 (*lane 3*), Oct4 (*lane 4*), Brn1 (*lane 6*), or Brn2 (*lane 7*). Note that there were supershifted bands in *lanes 2* and *7*. *D*, ^{32}P-labeled HRESF1 (1409/1441) probe was incubated with NE from P19 cells. EMSA was performed with the same amount of NE from P19 cells (5 μg). Specific gel-shifted bands (*5–7*) formed in P19EC cells and P19NPCs are indicated by *arrows*. *E*, a ^{32}P-labeled HRESF1 probe was incubated with NE from P19EC cells. The competition experiment was performed with 100-fold excess of unlabeled probe HRESF1 (*lane 2*) or the non-relevant probe CIE (*lane 3*). The supershift assay was performed with an antibody against SF1 (*lane 4*). Note that there were supershifted bands in *lanes 4*. *F*, *in vivo* occupancy of the *nestin* enhancer by different transcription factors. In ChIP assays, antibodies against Brn1, Brn2, Sox2, or SF1 were used to immunoprecipitate cross-linked chromatin fragments prepared from P19EC cells or P19NPCs. Immunoprecipitates were analyzed for the abundance of the *nestin* enhancer by quantitative PCR. The data were normalized relative to *nestin* enhancer occupancy by pre-immune IgG. *Ss*, supershift.

while the Oct2 antibody had no effect (Fig. 5*C*, *lanes 2–4*). In P19NPCs, formation of complex 3 was abolished by a Brn1 antibody, and complexes 3 and 4 were supershifted by a Brn2 antibody (Fig. 5*C*, *lanes 6* and 7). Complex 4 could be gradually supershifted with an increasing amount of Brn2 antibody when a series dilution of Brn2 antibody was performed (supplemental Fig. S1*A*, *lanes 6–8*). To determine whether Sox2 protein was present in these complexes, we compared the complexes formed with the nonspecific DNA competitor poly(dI-dC) (supplemental Fig. S1*A*, *lane 1*) *versus* poly(dG-dC) (supplemental Fig. S1*A*, *lanes 2–9*) with a longer exposure time. We found an additional band in the presence of poly(dG-dC) but not poly(dI-dC) (supplemental Fig. S1*A*, *lane 1 versus 2*). This complex could be supershifted with an antibody against Sox2 (supplemental Fig. S1*A*, *lane 9*). Together, these results indicate that the *cis*-element for POU factors was bound by Oct1 and Oct4 in P19EC cells, and Oct1, Brn1, and Brn2 in P19NPCs.

A time-course analysis of proteins binding to the HRESF1 probe was also performed (Fig. 5*D*). There were two bands (complexes 5 and 6) present in P19EC cells (A0), and the intensity of these bands gradually decreased upon neural differentiation. Meanwhile, the third band (complex 7) could be observed from R1 to R3 in P19NPCs. The specificity of the two bands in P19EC cells was

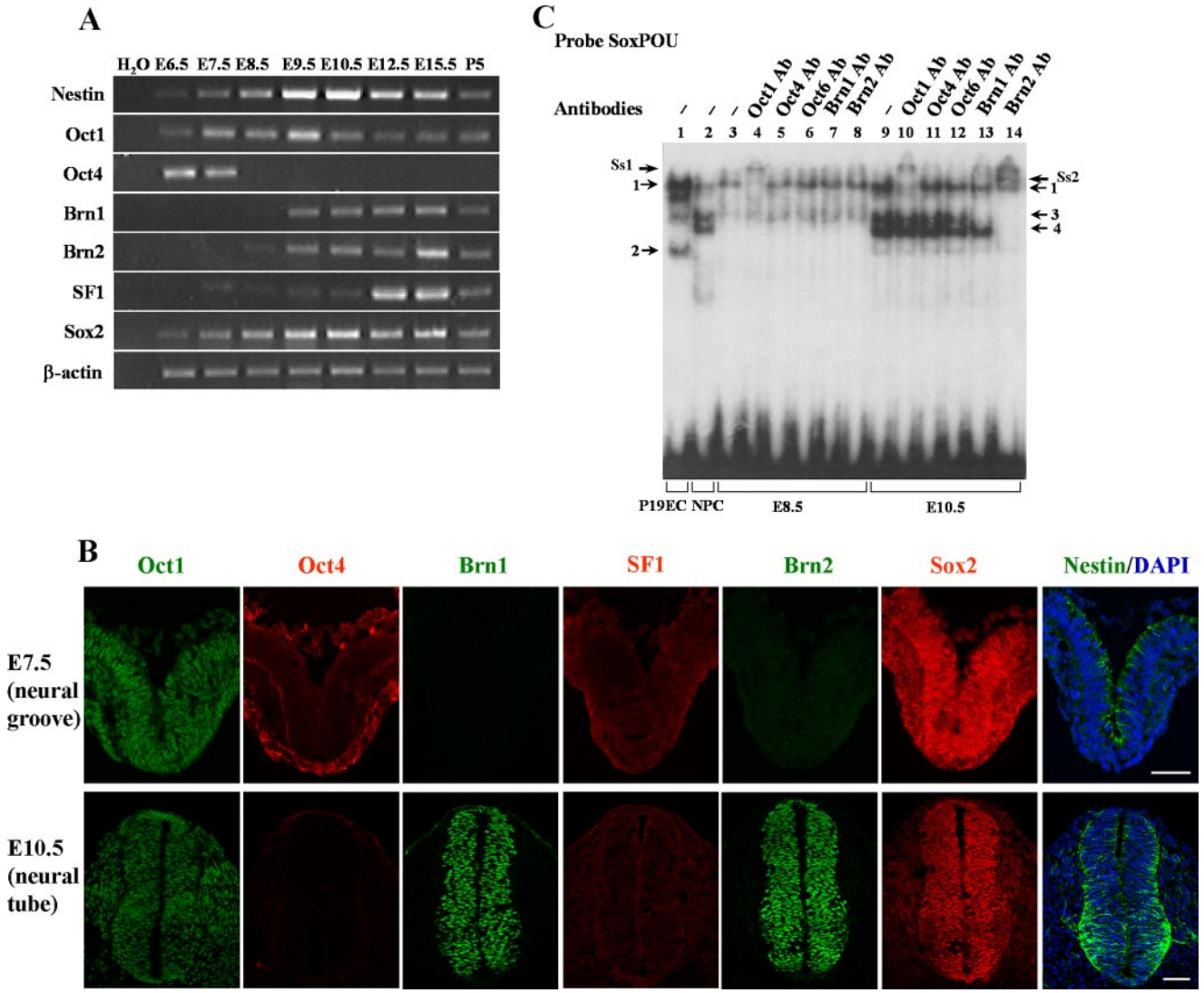

FIGURE 6. **Expression of SF1, Sox and POU family transcription factors in developing mouse embryos.** *A*, RT-PCR analysis for the expression of transcription factors. Total RNA extracted from mouse embryos at E6.5 and E7.5, mouse brain at E8.5, E9.5, E10.5, 12.5, and E15.5 or mouse cerebellum at P5 was used as the template for reverse transcription. Specific primers used for PCR amplifications are listed in supplemental Table S1. *B*, immunostaining of transcription factors was performed on transverse sections from E7.5 neural groove and E10.5 neural tube at the thoracic spinal level. *Bar*, 50 μm. *C*, a ^{32}P-labeled SoxPOU probe was incubated with NE from mouse embryos at E8.5 (*lanes 3–8*) or mouse brain at E10.5 (*lanes 9–14*). NE from P19EC cells or P19NPCs was used as a control (*lanes 1* and *2*). The supershift assay was performed with an antibody against Oct1 (*lanes 4* and *10*), Oct4 (*lanes 5* and *11*), Oct6 (*lanes 6* and *12*), Brn1 (*lanes 7* and *13*), or Brn2 (*lanes 8* and *14*). Gel-shifted bands are indicated by *arrows*.

confirmed by a competition assay (Fig. 5*E*, *lanes 1–3*), and the binding of SF1 protein to this probe was validated by the observation of a supershift with treatment with an SF1 antibody (Fig. 5*E*, *lane 4*). These data suggest that two overlapping SF1-binding sites recruit the SF1 protein in P19EC cells.

To further validate the binding of these transcription factors to the endogenous *nestin* gene enhancer, we immunoprecipitated chromatin from P19EC cells and P19NPCs with antibodies against Brn1, Brn2, Sox2, and SF1 (Fig. 5*F*). The precipitated chromatin was quantified by quantitative PCR with primers for the *nestin* enhancer, flanking the HRE-, POU-, Sox-, and SF1-binding sites. We found that the binding of Brn1 and Brn2 to the *nestin* enhancer was markedly enhanced in P19NPCs when compared with P19EC cells. In contrast, the levels of SF1 binding were high in P19EC cells and low in P19NPCs. The Sox2 protein bound to this enhancer in both P19EC and P19NPC cells. Together, these results suggest that different transcription factors are recruited to the endogenous *nestin* gene enhancer during the process of P19 cell neural differentiation: Sox2 and SF1 in undifferentiated P19EC cells, and Sox2, Brn1, and Brn2 in P19NPCs.

Different Transcription Factors Bind to the nestin Enhancer at Different Stages of Central Nervous System Development in Vivo—The above results led us to hypothesize that different transcription factors might be recruited to the *nestin* enhancer to regulate its expression during central nervous system development *in vivo*. To investigate this, we first examined the expression pattern of transcription factors in developing mouse embryos (Fig. 6). RT-PCR analysis showed that low levels of *nestin* mRNA were detected in E6.5 embryos, and *nestin* expression started to increase in E7.5 mouse embryos, with an expression peak in E9.5 and E10.5 mouse brains (Fig. 6*A*). *Oct1* was continuously expressed at all stages examined. *Oct4* was expressed at a high level in E6.5 embryos, but down-regulated at E7.5, and it ceased to be expressed from E8.5. In contrast, *Brn1* and *Brn2* were not

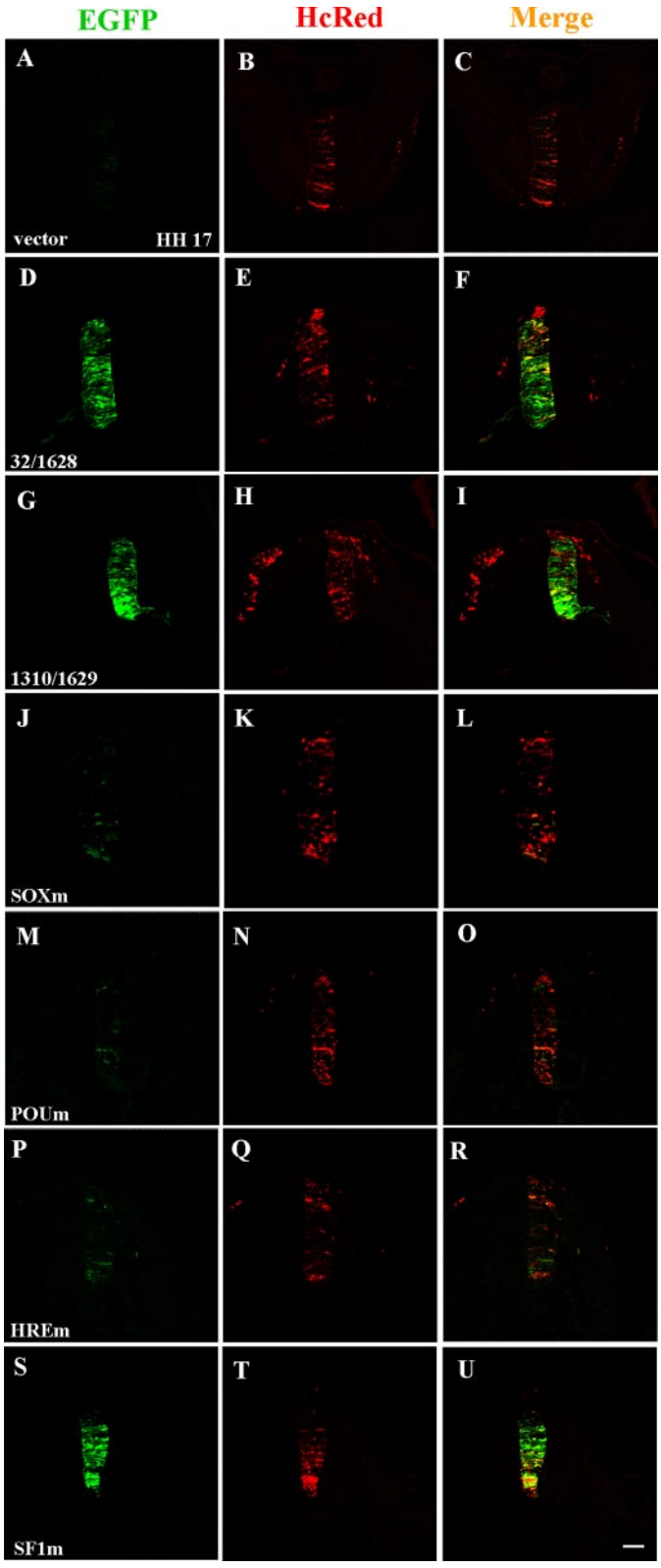

FIGURE 7. ***In vivo* characterization of the functional *cis*-elements in the second intron of the mouse *nestin* gene.** The pxtkEGFP vector containing a TK promoter and GFP coding sequence was used as a negative control. The second intron of the mouse *nestin* gene with wild-type or mutated *cis*-elements was placed upstream of the TK promoter to generate a series of GFP reporter gene constructs. The GFP constructs were electroporated into chick neural tubes together with the tracer plasmid, pHcRed1-N1, at HH stage 10. For *G* and *H*, a GFP construct and the tracer plasmid, pHcRed1-N1, were also injected and electroporated into the surrounding somite. The expressions of GFP and HcRed were detected 24 h later (at HH stage 17). Neural tubes expressing HcRed were selected and cut from chick embryos for cryosection, and the expression of GFP in the thoracic spinal cord was examined under a confocal microscope. The numbers of independent electroporated embryos that expressed GFP and HcRed for different constructs were as follows: 0/10 for the vector pxtkEGFP (*A–C*), 9/9 for the full-length second intron construct pxtkEGFP2In32/1628 (*D–F*), 30/31 for the 320-bp minimal enhancer construct pxtkEGFP2In1310/1629 (*G–I*), 5/21 for the Sox-mutated construct pxtkEGFP2InSOXm (*J–L*), 0/7 for the POU-mutated construct pxtkEGFP2InPOUm (*M–O*), 5/19 for the HRE-mutated construct pxtkEGFP2InHREm (*P–R*), and 13/13 for the SF1-mutated construct pxtkEGFP2InSF1m (*S–U*). *Bar*, 50 μm.

expressed in E6.5 and E7.5 embryos, and their expression was only initiated at E9.5. *SF1* was not expressed in E6.5 embryos, started to be expressed at a very low level from E7.5 to E10.5, and was up-regulated after E12.5. *Sox2* showed a very similar expression pattern to that of *nestin*, suggesting that Sox2 might regulate *nestin* transcription at both the neural plate and neural tube stages. Immunostaining was used to detect the pattern of protein expression of these transcription factors at the thoracic spinal level (Fig. 6*B*). Consistent with the RT-PCR results, the Oct1 protein was expressed in both the E7.5 neural fold and E10.5 neural tube. However, the levels of Oct4 protein expression were very low in the neural fold, and Oct4 expression was completely lost in the neural tube of E10.5 embryos. Brn1 and Brn2 were not expressed in E7.5 embryos, but these proteins were strongly and specifically expressed in E10.5 neural tube. Sox2 was expressed strongly in both the E7.5 neural fold and E10.5 neural tube. In contrast, weak expression of SF1 was detected in the E7.5 neural fold, and its expression was undetectable in the E10.5 neural tube.

To determine whether these transcription factors could bind to the *nestin* gene enhancer, we prepared nuclear extracts from E8.5 mouse embryos, E10.5 and E12.5 mouse brain, and performed EMSA with a radiolabeled SoxPOU probe. As shown in Fig. 6*C*, we could detect one band from E8.5 embryo nuclear extract, and this band could be supershifted by an Oct1 antibody, but not by any other antibodies (Fig. 6*C*, *lanes 3–8*). The nuclear extract of E10.5 mouse brain contained three major bands, one slowly migrating band, and two rapidly migrating duplicate bands (Fig. 6*C*, *lane 9*). Oct1 antibody could supershift the slowly migrating band, but antibodies against Oct4 and Oct6 had no effect (Fig. 6*C*, *lanes 10–12*). A Brn1 antibody supershifted the upper band of the duplex, and treatment with a Brn2 antibody eliminated both bands (Fig. 6*C*, *lanes 13* and *14*). Brn1 and Brn2 proteins in E12.5 brain and spinal cord could also bind to the SoxPOU probe (supplemental Fig. S1*B*). Due to a difficulty in collecting sufficient quantities of nuclear extracts, we were unable to perform the EMSA analysis with E6.5 and E7.5 embryos. Taken together, these results show that different transcription factors were expressed differently in the neural stem cells of the neural fold of E7.5 and the neural tube of E10.5 mouse embryos. These transcription factors were recruited to the *nestin* enhancer at different stages, Oct1 in the neural epithelium of E8.5 mouse embryos, and Oct1, Brn1, and Brn2 in the neural tube of E10.5 embryos.

Different cis-Elements within the nestin Enhancer Are Used in Chick Embryo Neural Tube Development—To further confirm the function of different *cis*-elements in the mouse *nestin* gene

enhancer during central nervous system development *in vivo*, we examined the enhancer activity in the neural tube of chick embryos. The wild-type and mutated enhancer-driven GFP reporter constructs were electroporated into one side of neural tube of chick embryos at HH stage 10, and GFP expression in the thoracic spinal cord was detected at HH stage 17. The HcRed1 expression vector was used as a tracer. We found that the expression vector itself could not induce GFP expression (Fig. 7, *A–C*), whereas the wild-type full-length enhancer (Fig. 7, *D–F*) or 320-bp minimal enhancer (Fig. 7, *G–I*) could activate strong GFP expression in the neural tube. However, this enhancer could not drive GFP expression in the surrounding somite, in which co-electroporated HcRed1 was expressed (Fig. 7, *G versus H*), indicating the neural tissue specificity of the *nestin* enhancer in chick embryos. Mutations of the *cis*-elements for Sox (Fig. 7, *J–L*), POU (Fig. 7, *M–O*), and HRE (Fig. 7, *P–R*) in the minimal enhancer greatly decreased GFP expression. In contrast, mutation of the SF1-binding sites did not disrupt reporter gene expression (Fig. 7, *S–U*). These results indicate that the Sox, POU, and HRE *cis*-elements are essential for *nestin* enhancer activity in the developing central nervous system, but SF1 sites were not functional in chick embryo neural tubes.

DISCUSSION

Nestin is a neural progenitor cell-specific marker, and its expression is strictly regulated during central nervous system development. Studies in transgenic mice showed that the central nervous system-specific enhancer of the human and rat *nestin* genes resides in the second intron (5, 16). In this study, we confirm that the second intron of the mouse *nestin* gene also contains a central nervous system-specific enhancer, because it can drive reporter gene expression in the developing central nervous system of transgenic mice (Fig. 1) and in the neural tube of chick embryos (Fig. 7). To reveal the molecular mechanisms of transcriptional regulation of the mouse *nestin* gene in neural progenitor cells, we took advantage of the neural differentiation program of mouse embryonic carcinoma P19 cells. Analogous to neural induction and neurogenesis *in vivo* (5, 16), *nestin* expression showed a transient up-regulation during P19 cell neural differentiation (Fig. 2). *nestin* expression was at a basal level in undifferentiated P19EC cells; the expression increased along with P19EC cells differentiated into P19NPCs and decreased when NPCs terminally differentiated into neurons and glial cells (Fig. 2). Luciferase assays showed that the second intron of the mouse *nestin* gene could induce a transient up-regulation of the reporter gene, which was reminiscent of the endogenous *nestin* expression during P19 cell neural differentiation (Fig. 2*E*). These results suggested that the neural differentiation of P19 cells could be used to study the function of *nestin* enhancer and to dissect the detailed mechanisms of *nestin* gene regulation *in vitro* and *in vivo*.

Series deletion analysis led to the identification of a minimal enhancer located in the 3′ 320-bp region of the second intron (Fig. 3*A*), and this minimal enhancer could also drive reporter gene expression in developing NPCs of transgenic mice (Fig. 1). Transgenic analysis showed that the 3′ 320-bp region in the second intron of the mouse *nestin* gene harbors a general central nervous system-specific enhancer for the *nestin* expression, similar to what have been reported in the human and rat *nestin* genes. By analogy, some regional expression of the mouse *nestin* gene might require other *cis*-elements outside of the 320-bp region (24–26). Like the 257-bp region of the rat *nestin* enhancer and the 120-bp region of the human *nestin* gene enhancer, this 320-bp region contains HRE-, Sox-, POU-, and SF1-binding sites (24–26). Mutations in all of these sites, except SF1, strongly reduced the enhancer activity of the mouse *nestin* gene in P19EC cells and P19NPCs (Fig. 3*D*), indicating that these sites are important to both the basal and central nervous system-specific enhancer activities of mouse *nestin* gene. Interestingly, mutations in two overlapping SF1-binding sites abolished enhancer activity in P19EC cells, but they had no effect on reporter gene expression in P19NPCs, suggesting that the SF1 sites are involved in basal enhancer activity in undifferentiated EC cells, but not in central nervous system-specific enhancer activity in NPCs. Consistently, chick embryo *in ovo* electroporation also showed that mutations in HRE, Sox, and POU sites caused a significant decrease in reporter gene expression, whereas mutations in the SF1-binding sites had no effect (Fig. 7). The central nervous system-specific enhancer with mutations in the SF1-binding sites could still drive reporter gene expression in the NPCs of E12.5 transgenic mice embryos.[4] These results support the notion that the functions of *cis*-elements in the central nervous system-specific enhancer are the same in P19NPCs as in the developing central nervous system *in vivo*.

The EMSA time-course analysis showed that different protein-DNA-binding complexes were formed for the Sox-POU and HRE-SF1 probes during P19 cell neural differentiation (Fig. 5). A reasonable hypothesis is that different transcription factors expressed at different stages of neural differentiation bind to these *cis*-elements to regulate *nestin* gene expression. To address this possibility, we performed supershift assays and found that oligonucleotides containing Sox- and POU-binding sites were bound by Oct1 and Oct4 proteins in P19EC cells but by the Oct1, Brn1, and Brn2 factors in P19NPCs (Fig. 5). The observation that the same POU-binding site is occupied by different POU factors at different differentiation stages is very interesting. The *Sox2* gene also showed a similar regulation mechanism, where its upstream promoter was bound by the Oct4 protein in embryonic stem cells and by Brn1 and Brn2 in NPCs (49). The probe that contains the HRE- and SF1-binding sites was bound by SF1 and unidentified protein(s) in P19EC cells and by different protein(s) in P19NPCs (Fig. 5). It has been reported that a variety of nuclear hormone receptors are able to bind to the *nestin* enhancer, including the thyroid hormone receptor, retinoic acid receptor, retinoid X receptor, and chicken ovalbumin upstream promoter-transcription factor, and these receptors may have positive or negative effects upon *nestin* expression (25). Consistent with the EMSA results, ChIP assays confirmed binding of the Sox2 and SF1 proteins to the *nestin* enhancer in P19EC cells and also confirmed binding of Brn1, Brn2, and Sox2 in P19NPCs (Fig. 5). However, we were

[4] Z. Jin and N. Jing, unpublished observation.

unable to detect any Sox2 binding to the SoxPOU probe in the EMSA assay, and the ChIP analysis did not indicate that the Oct1 and Oct4 proteins were recruited to the *nestin* enhancer. One possible explanation for the absence of Sox2 binding may be that our EMSA conditions do not favor the formation of the Sox2-DNA complex, even though poly(dG-dC) was used instead of poly(dI-dC) (48).

Our observations suggest that regulation of the expression of the mouse *nestin* gene during P19 cell neural differentiation may recapitulate the events in the developing central nervous system *in vivo*. To test this possibility, we examined the expression pattern of putative transcription factors during the neural development of mouse embryos and found that the expression patterns of transcription factors were very similar to those observed during the neural differentiation of P19 cells (Figs. 4 and 6). EMSA assays also showed that the *nestin* enhancer could be bound by different transcription factors at different developmental stages, *e.g.* Oct1 in E8.5 and Oct1, Brn1, and Brn2 in E10.5 and E12.5 mouse embryos (Fig. 6 and supplemental Fig. S1*B*). Consistently, Miyagi *et al.* showed the binding of Brn1, Brn2, and Sox2 to the *nestin* enhancer in E12.5 brain and spinal cord using ChIP assays (50). Difficulties obtaining sufficient quantities of tissue prevented us from performing EMSA and ChIP assays from early mouse embryo stages, because our efforts to detect transcription factor occupancy at these stages of development were not successful.

Cultured cell lines often resemble particular cell types found in part of the embryonic anatomy at a certain developmental stage. P19EC cells are derived from a teratocarcinoma formed after transplantation of a 7.5 days post coitum embryo into testis (51), and they have a number of features in common with cells of the epiblast (52). Interestingly, an *Oct4*/*lacZ* transgenic study revealed two regulatory elements in the *Oct4* gene: one drives *Oct4* expression in preimplantation embryos and is specifically active in embryonic stem and embryonic germ cells; the other directs the epiblast-specific expression pattern, and its activity is restricted to P19EC cells (53). Consistently, we found that P19EC cells express epiblast marker FGF5, and a high population of P19EC cells could be converted into neural stem cells in N2B27 serum-free medium. We further showed that N2B27-induced neural stem cells bear anterior neuroectoderm characters and could be efficiently caudalized by RA (54). Therefore, the P19NPCs generated from RA-treated P19EC cells likely are the neural progenitors of the caudal nervous system, *i.e.* the hindbrain and spinal cord.

It has been proposed previously that a change in POU proteins expression is required for the acquisition of neural potential (24). For the *nestin* gene, which is a molecular marker for neural progenitors, we provide evidence here that the *cis*-element for POU factors was bound by Oct1 and Oct4 in P19EC cells, and Oct1, Brn1, and Brn2 in P19NPCs. The observation that a same DNA regulatory element could be bound by different members of POU family strongly supports the idea that a switch for POU proteins works in controlling gene regulation. A recent study showed that *nestin* is regulated in a cell-cycle-dependent manner: the cell-cycle-dependent phosphorylation of an upstream regulator, Brn2, reduces its binding activity to the *nestin* core enhancer element and is responsible for the decreased *nestin* transcription in G_2-M phase (55). This line of evidence suggests a scenario that the absence of *nestin* expression in postmitotic neurons may simply be due to the lack of Brn2 activity.

In conclusion, we identified a central nervous system-specific enhancer in the 3′ region of the second intron of the mouse *nestin* gene. This region could drive reporter gene expression in the NPCs of the developing nervous system of transgenic mice and regulate *nestin* expression during P19 cell neural differentiation. The HRE, Sox, and POU *cis*-elements in this enhancer are important for *nestin* gene expression in NPCs *in vitro* and *in vivo*. Different transcription factors regulate *nestin* gene expression during P19 cell neural differentiation and central nervous system development. Sox2 and SF1 may mediate basal *nestin* expression in undifferentiated P19EC cells, whereas Sox2, Brn1, and Brn2 are recruited to maintain *nestin* expression in P19NPCs. Different factors were recruited to the *nestin* enhancer at different stages of mouse embryo development, Oct1 in E8.5 neural fold and Oct1, Brn1 and Brn2 in the neural tube at E10.5. Our studies therefore provide evidence that a temporal combination of transcription factors bind to the central nervous system-specific enhancer of *nestin* gene and control its expression.

Acknowledgments—We thank Dr. U. Lendahl for pSaStk/lacZ vector, Dr. H. Kondoh for ptkEGFP vector and Sox2 antibody, and Dr. K. Morohashi for the SF1 antibody.

REFERENCES

1. Itoh, K., and Sokol, S. Y. (2007) in *Principles of Developmental Genetics* (Moody, S. A., ed) pp. 241–257, Elsevier Inc., Academic Press, Burlington, MA
2. Dahlstrand, J., Lardelli, M., and Lendahl, U. (1995) *Brain Res. Brain Res. Rev.* **84,** 109–129
3. Lendahl, U., Zimmerman, L. B., and McKay, R. D. (1990) *Cell* **60,** 585–595
4. Wiese, C., Rolletschek, A., Kania, G., Blyszczuk, P., Tarasov, K. V., Tarasova, Y., Wersto, R. P., Boheler, K. R., and Wobus, A. M. (2004) *Cell. Mol. Life Sci.* **61,** 2510–2522
5. Zimmerman, L., Parr, B., Lendahl, U., Cunningham, M., McKay, R., Gavin, B., Mann, J., Vassileva, G., and McMahon, A. (1994) *Neuron* **12,** 11–24
6. Frederiksen, K., and McKay, R. D. (1988) *J. Neurosci.* **8,** 1144–1151
7. Gu, H., Wang, S., Messam, C. A., and Yao, Z. (2002) *Brain Res.* **943,** 174–180
8. Dahlstrand, J., Collins, V. P., and Lendahl, U. (1992) *Cancer Res.* **52,** 5334–5341
9. Frisen, J., Johansson, C. B., Torok, C., Risling, M., and Lendahl, U. (1995) *J. Cell Biol.* **131,** 453–464
10. Lenka, N., Lu, Z. J., Sasse, P., Hescheler, J., and Fleischmann, B. K. (2002) *J. Cell Sci.* **115**, 1471–1485
11. Smukler, S. R., Runciman, S. B., Xu, S., and van der Kooy, D. (2006) *J. Cell Biol.* **172,** 79–90
12. Jin, Z. G., Liu, L., Zhong, H., Zhang, K. J., Chen, Y. F., Bian, W., Cheng, L. P., and Jing, N. H. (2006) *Acta Biochim. Biophys. Sin.* **38,** 207–212
13. Chou, Y. H., Khuon, S., Herrmann, H., and Goldman, R. D. (2003) *Mol. Biol. Cell* **14,** 1468–1478
14. Sahlgren, C. M., Mikhailov, A., Vaittinen, S., Pallari, H. M., Kalimo, H., Pant, H. C., and Eriksson, J. E. (2003) *Mol. Cell. Biol.* **23,** 5090–5106
15. Wakamatsu, Y., Nakamura, N., Lee, J. A., Cole, G. J., and Osumi, N. (2007) *Development* (*Camb.*) **134,** 2425–2433
16. Lothian, C., and Lendahl, U. (1997) *Eur. J. Neurosci.* **9,** 452–462
17. Dubois, N. C., Hofmann, D., Kaloulis, K., Bishop, J. M., and Trumpp, A. (2006) *Genesis* **44,** 355–360

18. Isaka, F., Ishibashi, M., Taki, W., Hashimoto, N., Nakanishi, S., and Kageyama, R. (1999) *Eur. J. Neurosci.* **11,** 2582–2588
19. Petersen, P. H., Zou, K., Hwang, J. K., Jan, Y. N., and Zhong, W. (2002) *Nature* **419,** 929–934
20. Tronche, F., Kellendonk, C., Kretz, O., Gass, P., Anlag, K., Orban, P. C., Bock, R., Klein, R., and Schutz, G. (1999) *Nat. Genet.* **23,** 99–103
21. Kawaguchi, A., Miyata, T., Sawamoto, K., Takashita, N., Murayama, A., Akamatsu, W., Ogawa, M., Okabe, M., Tano, Y., Goldman, S. A., and Okano, H. (2001) *Mol. Cell. Neurosci.* **17,** 259–273
22. Mignone, J. L., Kukekov, V., Chiang, A. S., Steindler, D., and Enikolopov, G. (2004) *J. Comp. Neurol.* **469,** 311–324
23. Yamaguchi, M., Saito, H., Suzuki, M., and Mori, K. (2000) *Neuroreport* **11,** 1991–1996
24. Josephson, R., Muller, T., Pickel, J., Okabe, S., Reynolds, K., Turner, P. A., Zimmer, A., and McKay, R. D. (1998) *Development* (*Camb.*) **125,** 3087–3100
25. Lothian, C., Prakash, N., Lendahl, U., and Wahlstrom, G. M. (1999) *Exp. Cell Res.* **248,** 509–519
26. Yaworsky, P. J., and Kappen, C. (1999) *Dev. Biol.* **205,** 309–321
27. Tanaka, S., Kamachi, Y., Tanouchi, A., Hamada, H., Jing, N., and Kondoh, H. (2004) *Mol. Cell. Biol.* **24,** 8834–8846
28. Yang, J., Cheng, L., Yan, Y., Bian, W., Tomooka, Y., Shiurba, R., and Jing, N. (2001) *Biochim. Biophys. Acta* **1520,** 251–254
29. Yang, J., Bian, W., Gao, X., Chen, L., and Jing, N. (2000) *Mech. Dev.* **94,** 287–291
30. Cheng, L. P., Yang, J., and Jing, N. H. (2000) *Acta Biochim. Biophys. Sin.* **32,** 649–652
31. Cheng, L., Jin, Z., Liu, L., Yan, Y., Li, T., Zhu, X., and Jing, N. (2004) *FEBS Lett.* **565,** 195–202
32. Hou, Q., Gao, X., Zhang, X., Kong, L., Wang, X., Bian, W., Tu, Y., Jin, M., Zhao, G., Li, B., Jing, N., and Yu, L. (2004) *Eur. J. Neurosci.* **20,** 1593–1603
33. Uchikawa, M., Ishida, Y., Takemoto, T., Kamachi, Y., and Kondoh, H. (2003) *Dev. Cell* **4,** 509–519
34. Gao, X., Bian, W., Yang, J., Tang, K., Kitani, H., Atsumi, T., and Jing, N. (2001) *Biochem. Biophys. Res. Commun.* **284,** 1098–1103
35. Tang, K., Yang, J., Gao, X., Wang, C., Liu, L., Kitani, H., Atsumi, T., and Jing, N. (2002) *Biochem. Biophys. Res. Commun.* **293,** 167–173
36. Yan, Y., Bian, W., Xie, Z., Cao, X., Le Roux, I., Guillemot, F., and Jing, N. (2004) *Dev. Dyn.* **231,** 248–257
37. Hamburger, V., and Hamilton, H. L. (1951) *J. Morphol.* **88,** 49–92
38. Leers-Sucheta, S., Morohashi, K., Mason, J. I., and Melner, M. H. (1997) *J. Biol. Chem.* **272,** 7960–7967
39. Tomooka, Y., Kitani, H., Jing, N., Matsushima, M., and Sakakura, T. (1993) *Proc. Natl. Acad. Sci. U. S. A.* **90,** 9683–9687
40. Bain, G., Ray, W. J., Yao, M., and Gottlieb, D. I. (1994) *BioEssays* **16,** 343–348
41. Wang, C., Xia, C., Bian, W., Liu, L., Lin, W., Chen, Y. G., Ang, S. L., and Jing, N. (2006) *Mol. Biol. Cell* **17,** 3075–3084
42. Bai, G., Sheng, N., Xie, Z., Bian, W., Yokota, Y., Benezra, R., Kageyama, R., Guillemot, F., and Jing, N. (2007) *Dev. Cell* **13,** 283–297
43. Ding, S., Wu, T. Y., Brinker, A., Peters, E. C., Hur, W., Gray, N. S., and Schultz, P. G. (2003) *Proc. Natl. Acad. Sci. U. S. A.* **100,** 7632–7637
44. Lonigro, R., Donnini, D., Zappia, E., Damante, G., Bianchi, M. E., and Guazzi, S. (2001) *J. Biol. Chem.* **276,** 47807–47813
45. Pelizzoli, R., Tacchetti, C., Luzzi, P., Strangio, A., Bellese, G., Zappia, E., and Guazzi, S. (2008) *Int. J. Dev. Biol.* **52,** 55–62
46. Barnea, E., and Bergman, Y. (2000) *J. Biol. Chem.* **275,** 6608–6619
47. Kamachi, Y., Uchikawa, M., and Kondoh, H. (2000) *Trends Genet.* **16,** 182–187
48. Dailey, L., Yuan, H., and Basilico, C. (1994) *Mol. Cell. Biol.* **14,** 7758–7769
49. Catena, R., Tiveron, C., Ronchi, A., Porta, S., Ferri, A., Tatangelo, L., Cavallaro, M., Favaro, R., Ottolenghi, S., Reinbold, R., Scholer, H., and Nicolis, S. K. (2004) *J. Biol. Chem.* **279,** 41846–41857
50. Miyagi, S., Nishimoto, M., Saito, T., Ninomiya, M., Sawamoto, K., Okano, H., Muramatsu, M., Oguro, H., Iwama, A., and Okuda, A. (2006) *J. Biol. Chem.* **281,** 13374–13381
51. McBurney, M. W., and Rogers, B. J. (1982) *Dev. Biol.* **89,** 503–508
52. Robertson, E. J. (1987) *Teratocarcinomas and Embryonic Stem Cells: A Practical Approach*, IRL Press, Oxford/Washington DC
53. Yeom, Y. I., Fuhrmann, G., Ovitt, C. E., Brehm, A., Ohbo, K., Gross, M., Hubner, K., and Scholer, H. R. (1996) *Development* (*Camb.*) **122,** 881–894
54. Xia, C., Wang, C., Zhang, K., Qian, C., and Jing, N. (2007) *Differentiation* **75,** 912–927
55. Sunabori, T., Tokunaga, A., Nagai, T., Sawamoto, K., Okabe, M., Miyawaki, A., Matsuzaki, Y., Miyata, T., and Okano, H. (2008) *J. Cell Sci.* **121**, 1204–1212